Evaluation of harmonic methods for calculating the free energy of defects in solids

Stephen M. Foiles
Sandia National Laboratories, Livermore, California 94551-0969
(Received 13 September 1993)

The free energy of defects in solids is computed with Monte Carlo simulation techniques and by various approximate techniques. The results are compared in order to determine the accuracy and range of applicability of the various approximate methods. The systems studied are a bulk crystal, a vacancy, a (100) free surface, and a $\Sigma 5(310)/[001]$ symmetric tilt boundary in Cu described by embedded-atom method potentials. The Monte Carlo simulations employ both the Frenkel-Ladd method and thermodynamic integration. The approximate techniques include quasiharmonic calculations and the recently proposed local harmonic method. The results indicate that the harmonic methods significantly underestimate the temperature variation of the defect-free energies for this potential. The discrepancies become large for temperatures above about half of the melting point.

I. INTRODUCTION

The knowledge of the free energy of defects is important in the predicting many physical phenomena. One example is in nucleation theory. The free energy of the interface between the two phases in question is a crucial ingredient in determining the barrier to nucleation and nucleation rates. However, the determination of free energies from atomic scale computer simulations is a difficult task. In this paper, the accuracy of approximate methods of determining the free energy in atomic scale simulations will be compared to accurate Monte Carlo (MC) simulation results. The goal is to provide a measure of the accuracy and range of applicability of these approximate methods.

The calculation of the free energy is substantially more difficult than the calculation of the energy or enthalpy of a defect. The zero-temperature defect energy can be computed readily from assumed interatomic potentials by molecular statics or energy minimization techniques. Zero-temperature defect energies can also be computed from first-principles electronic structure calculations. Finite-temperature properties of a defect system can be computed from MC simulations. MC simulations provide a means of computing the ensemble average of a quantity. Thus, any quantity that can be written as an ensemble average can be computed in a straightforward manner, though the simulations may require substantial amounts of computer time to obtain reliable statistics. The free energy, though, cannot be written as a simple ensemble average. Therefore, more elaborate techniques are required to compute the defect-free energies. The free energy and/or free-energy differences can be computed via a variety of techniques that have been proposed.[1-7] All of these methods have the disadvantage that the computational effort required is very large.

One method of simplifying the computational problem is to introduce the quasiharmonic approximation.[8] In this approach the full Hamiltonian is replaced by a harmonic expansion about the equilibrium positions. The vibrational frequencies can then be computed by diagonalization of the dynamical matrix and the thermodynamic functions can be computed from these frequencies. There are two potential shortcomings with this approach. First, the harmonic approximation may not be valid at higher temperatures. Previous calculations[9] using the potentials considered here showed that the thermodynamic properties of the bulk lattice are well represented by quasiharmonic results. The quasiharmonic approximation can break down for two reasons. First, the amplitude of the vibrations can become large enough that the quadratic approximation of the potential energy breaks down. This breakdown may be more severe at a defect. For a crystal with inversion symmetry, the third-order terms in the expansion of the potential energy must vanish by symmetry. Thus, the anharmonic corrections will enter at fourth order. At a defect, the third-order terms need not vanish, so the harmonic approximation is more suspect for a defect environment than for a perfect crystal. The second reason that the harmonic approximation can fail is the onset of diffusive processes. Again, this is more likely to occur at extended defects such as grain boundaries or dislocation cores than in the bulk. Thus, even though the harmonic approximation has been seen to be good for the bulk crystal, it is an open question whether it works well at a defect.

The other drawback to quasiharmonic (QH) calculations of the free energy of large defects is the computational effort required. While these calculations are faster than MC simulations, the work required to determine the eigenfrequencies by standard techniques scales as N^3, where N is the number of atoms in the periodic cell for the calculation. (This scaling is softened for intermediate size systems due to the fact that the number of points in the Brillouin zone that must be sampled scales as N^{-1} until one gets down to a single k point.) This factor makes the direct application of quasiharmonic calculations to large defects computationally very intensive.

The potentially large computational effort associated with quasiharmonic calculations has prompted efforts to find computationally simpler models. LeSar, Najafabadi, and Srolovitz[10] and Sutton[11] have both proposed free-energy models based on a local estimate of the phonon density of states. The method proposed by LeSar *et al.* is

referred to as the local harmonic (LH) method. These models are described in detail below. They have been used to compute grain boundary free energies,[12] and segregation of binary alloys to interfaces.[13,14] The latter application also involves making approximation to the configurational entropy and defining effective interactions for the case of alloys at finite concentrations. These methods have been reviewed by Sutton.[15]

The main goal of this paper is to provide some comparisons between the approximate results obtained with the QH and LH methods and the MC results. There have been some previous comparisons of the LH method to MC-based results. The perfect crystal free energy and equilibrium volumes for a Morse potential were found to be in good agreement.[10] For a monovacancy, the temperature variation predicted by the LH approximation was about 20% smaller than that obtained from the MC simulations. In addition, the perfect crystal free energy and entropy of bulk Au described by embedded-atom method (EAM) potentials was found to be well described by the LH approximation.[12] For the case of the interfacial segregation, the segregation profiles computed from MC simulations have been compared to results based in part on the LH approximation.[13,14] These comparisons do not provide a clean test of the LH approximation since they also introduce a point approximation to the entropy and the definition of effective interactions in the alloy case. A direct test of the LH approximation for the case of substitutional impurities has been performed by Rittner, Foiles, and Seidman.[16] In this study the segregation free energy of single impurities near surfaces and grain boundaries were computed both with the LH approximation and using the method of overlapping distributions.[3] It was found that the LH approximation was accurate in most cases, though for impurities with a substantial size mismatch with the host lattice, there are significant errors associated with the LH approximation.

In the present paper, the free energy of a perfect crystal, a monovacancy, a (100) surface, and a $\Sigma 5$ (310)/[001] symmetric tilt boundary are computed via MC simulation methods, via QH calculations and via LH calculations. These results will provide a benchmark for judging the accuracy of QH calculations compared to MC results and of the accuracy of the LH calculations as an approximation to the QH method. The latter comparison has also been studied by Rickman and Srolovitz[17] and by Zhao, Najafabadi, and Srolovitz.[18] In both of these papers, extensions of the local harmonic model designed to bring it into better agreement with the quasiharmonic model are presented. These extensions are not addressed in this paper.

The paper is organized as follows. In the next section, the details of the MC simulations and the QH and LH calculations are discussed. In Sec. III, the numerical results of the calculations will be presented and the last section will discuss the results.

II. CALCULATIONAL DETAILS

All of the calculations are performed using embedded-atom method[19] interatomic potentials for Cu.[20] The EAM is a semiempirical approximation for the total energy of a metallic system which has been shown in previous work to provide a good description of the noble metals.[21] The computational effort required to compute the total energy and forces with this method are comparable to but somewhat greater than that required for the use of simple pair interactions. The calculational effort required to compute the second and third derivatives of the total energy that are needed by the methods described below is substantially greater for the EAM than for pair methods. The intent of this paper is not to test the ability of the EAM to describe real Cu, but rather to compare the predictions of various simulation techniques for a model of the energetics which is qualitatively similar to that of a real metal.

A. Monte Carlo simulation methods

The Monte Carlo simulations will be based on thermodynamic integration and the Frenkel-Ladd (FL) method.[4] The FL technique will be used to obtain the free energy at intermediate temperatures. As will be discussed below, the FL method does not work well at high temperatures. The high-temperature free energies will be obtained by computing the enthalpy of the defect at a variety of temperatures and fitting these results to an appropriate functional form. This enthalpy can then be used to compute the variation of the free energy with temperature from the relation

$$\frac{d}{dT}\left[\frac{G}{T}\right]=-\frac{H}{T^2}\ , \tag{1}$$

where G and H are the free energy and enthalpy and T is the temperature. The results of FL simulations performed at moderate temperatures will be used as the starting point for this integration.

The computation of the enthalpy can be performed using standard MC techniques. The difficulty lies in obtaining sufficient statistical accuracy. The thermodynamic properties of the defect are related to excess quantities at the defect. This is the difference between the enthalpy of the system with the defect and the enthalpy of the same number of atoms in a perfect crystal. This difference can be smaller than the magnitude of the fluctuations in the enthalpy. Thus, long simulations are required in order to obtain meaningful statistics for the excess enthalpy and therefore the free energies. This problem is most severe for the vacancy, since most of the simulation cell has properties very close to those of the bulk crystal. The boundary conditions used for these simulations are constant volume or constant area in the case of slab geometries. The volume is determined from the equilibrium lattice constant determined for that temperature using constant pressure MC simulations that have been run previously. This will then give simulations that are essentially at constant zero pressure. There is a deficiency inherent in these simulations, though. The number of atoms in the simulation is held fixed, so that the system is not free to form vacancies (other than in Frankel pairs) as should be allowed to occur in the real system. This problem has been discussed in detail for the case of bulk free-

energy simulations by Swope and Andersen.[22] The free energies obtained here should be above the true free energy, since the constant particle number acts as a constraint on the system preventing it from reaching the absolute free-energy minimum state. As will be seen, the free energy which we obtain from the MC simulations will be less than that obtained from the harmonic methods. Therefore, allowing the number of atoms to vary in the simulations would increase the disagreement between the MC results and the harmonic model results.

The FL method[4] relies on an exact property of the free energy. Consider a Hamiltonian, $H(\lambda)$, which depends on some parameter λ. In can be shown that

$$\frac{dF}{d\lambda}=\left\langle\frac{dH}{d\lambda}\right\rangle_{\lambda}, \tag{2}$$

where $F(\lambda)$ is the free energy associated with $H(\lambda)$. In this expression, the brackets refer to the ensemble average corresponding to the Hamiltonian $H(\lambda)$. The parametrized Hamiltonian can be taken to be

$$H(\lambda)=(1-\lambda)H_{\text{ref}}+\lambda H , \tag{3}$$

where H is the desired Hamiltonian and H_{ref} is a reference Hamiltonian whose free energy is assumed to be known. The expectation value of $dH/d\lambda$ is computed for various values of λ by standard MC techniques and Eq. (2) used to compute $F(1)$ relative to the known $F(0)$. In the FL method, the reference Hamiltonian, H_{ref}, is taken to be a system of independent harmonic oscillators with each oscillator centered near the equilibrium position of an atom. The free energy of a system of harmonic oscillators is readily calculated from standard formulas.[8] Assuming that the integration of Eq. (2) is performed accurately, this will give the desired free energy.

There are two technical complications to using this approach in the present case. The first problem arises for any Hamiltonian which has translational symmetry. There are really only $3(N-1)$ relevant positional degrees of freedom. Note that the reference Hamiltonian does not have translational symmetry. Thus, when one calculates the average at $\lambda=1$, the expectation value of $dH/d\lambda$ will diverge since the system can translate freely according to $H(1)$ but such translation will yield arbitrarily large negative values of $dH/d\lambda=H(1)-H(0)$. This makes the accurate integration of Eq. (2) impractical. The solution to this problem used here is to add a term to $H(1)$ which couples the center of mass of the system to a harmonic potential. This prevents this free translation. The free energy associated with this coupling to the harmonic potential can be readily computed and the value of $F(1)$ adjusted to compensate for this addition.

The second problem with applying the FL method represents a more fundamental limitation of the approach. At high temperatures, diffusive behavior and/or the creation of thermal defects will occur in the system. In this case, the energy associated with the reference Hamiltonian becomes very large. Since the reference Hamiltonian strongly penalizes these variations, they will only occur for λ near 1. This again makes the integration of Eq. (2) impractical since the expectation value of $dH/d\lambda$ will vary rapidly at $\lambda=1$. This is potentially a much more serious problem for defect structures than for bulk simulations as is evidenced by the fact that grain boundary diffusion is much larger than bulk diffusion. This latter problem will be seen to limit the range of temperatures for which the FL method can be applied and is the reason for using thermodynamic integration for the high-temperature results.

In summary, the free energy is determined by the FL method for 500 K. This is above the Debye temperature of Cu so that quantum effects are small and is below the temperature where the above problems with the FL method arise. Standard MC calculations are then used to determine the enthalpy as a function of temperature. These data are fit to a low-order polynomial, typically cubic. This enthalpy data is used in conjunction with Eq. (1) to determine the free energy for all other temperatures.

B. Quasiharmonic calculations

In the harmonic approximation, a quadratic expansion of the potential energy is made about the equilibrium positions. The vibrational modes and frequencies of the lattice can then be computed by diagonalizing the dynamical matrix as described in the literature.[8,23] The thermodynamic functions can then be readily computed in terms of a sum over the vibrational modes or equivalently by an integration over the vibrational density of states. In particular, the free energy is given by

$$F=k_BT\sum_j \ln\left[2\sinh\frac{h\nu_j}{2k_BT}\right] . \tag{4}$$

In this equation, ν is the vibrational frequency and the index j refers to the different modes. In the case of periodic systems, it also includes the sum over the Brillouin zone. In the high-temperature or classical limit, this expressions simplifies to

$$F_{\text{cl}}=k_BT\sum_j \ln\left[\frac{h\nu_j}{k_BT}\right] , \tag{5}$$

where the subscript cl refers to the classical limit.

It is, in principle, possible to relax the atomic positions in quasiharmonic calculations so as to minimize the total free energy. Sutton[15] has presented the explicit expression for the force due to the free-energy contributions in the QH approximation. Unfortunately, this expression is difficult to implement in practice since it requires the evaluation of the third derivatives of the energy with respect to position. For the EAM potential used here, it is conceptually simple to write down the analytic expressions for the third derivatives, however, the computational and programming effort required to implement these terms is large. This is due to the fact that the determination of the third derivative of the energy of atom i requires a sum over the neighbors of the neighbors of atom i. This substantially increases the effort relative to simple pair interactions.

For this reason, the position in the QH calculations have not been optimized to minimize the free energy.

The positions are determined as follows. First, the QH lattice constant of the bulk material is determined for the desired temperature. Next, the equilibrium atomic positions at 0 K are determined by energy minimization. Finally, the coordinates are uniformly expanded to the QH lattice constant. The resulting structure is then used in the QH calculation of the defect energy. This procedure ignores the fact that the coordinates around the defect will have a different thermal expansion than the bulk. The quantitative consequences of this have been explored in a couple of test cases by manually adjusting the coordinates near the defect to find a better free-energy minimum. These tests, which will be discussed below, indicate that the change in the free energy of the defect due to this further refinement of the structure is small.

C. Local harmonic calculations

The idea behind the local harmonic approximation[10,11] is to eliminate the need to perform the diagonalization of the $3N\times 3N$ matrix. Instead, each atom is treated as an Einstein oscillator. The frequencies associated with each atom are determined by frequencies of the atom moving in the potential of the remaining atoms fixed at their equilibrium position. This reduces the problem to the diagonalization of N 3×3 matrices.

An alternative way to viewing the local harmonic approximation is to consider the moments of the density of states. The moment theorem[24] of Cryot-Lackmann shows that second moment of the vibrational density of states projected onto an atom i and direction α can be related to the diagonal elements of the dynamical matrix:

$$\mu_{i\alpha}^{(2)}=\int_0^\infty \omega^2 n_{i\alpha}(\omega)d\omega=D_{i\alpha,i\alpha}\ , \tag{6}$$

where $n_{i\alpha}$ is the density of states projected onto atom i and direction α, and $D_{i\alpha,i\alpha}$ is the corresponding diagonal element of the dynamical matrix. The directions, α, associated with each atom are chosen such that the 3×3 matrix $D_{i\alpha,i\beta}$ is diagonal. The local harmonic approximation is obtained by modeling the local density of states, $n_{i\alpha}(\omega)$, by a δ function such that the second moment is correct. This leads to a free energy given by

$$\frac{F_{\rm LH}}{k_BT}=\sum_{i\alpha}\ln 2\sinh\frac{h\sqrt{\mu_{i\alpha}^{(2)}}}{4\pi k_BT}\approx\sum_{i\alpha}\ln\frac{h\sqrt{\mu_{i\alpha}^{(2)}}}{2\pi k_BT}\ . \tag{7}$$

The second expression is the value in the high-temperature classical limit. In most of the applications of the LH approximation,[10,12–14] the high-temperature form is used. In that case, the expression for the free energy can be cast in terms of the determinant of the 3×3 submatrices associated with each atom. This avoids the need to diagonalize the 3×3 matrices, however, it restricts the application of the method to the classical limit. In the results presented here, the full quantum-mechanical expression is used.

Other expressions for the free energy can be generated based on the second moment by assuming different functional forms for the density of states. This has been done by Sutton.[11,15] A related approximation is discussed in the Appendix. The different forms assumed for the density of states gives results for the free energy which differ from each other in the high-temperature limit by a constant times the temperature. In the determination of the defect energies of interest here, this constant cancels out and so the different models of the density of states yield the same defect free energy. Thus, we will present results for the LH model both because it is the simplest and it is the most commonly used. The consequences of different forms assumed for the bulk thermodynamics are discussed in the Appendix.

The free energy can be minimized by consideration of the effective forces associated with the free energy. This is accomplished by taking the derivative of the free energy in Eq. (7) with respect to particle positions. Since the dynamical matrix is itself given by the second derivatives of the energy with respect to positions, the calculation of the force associated with the free energy requires the evaluation of a subset of the third derivatives of the energy with respect to position. As mentioned earlier, this greatly increases the computational effort for EAM-like energy expression over the calculation of the free energy or the zero-temperature forces.

III. RESULTS

A. Bulk lattice

The equilibrium lattice constant and free energy of the perfect fcc crystal have been computed as a function of temperature via the various methods that have been discussed above. The results shown are for temperatures above 300 K, which is close to the Debye temperature for Cu, so that quantum effects will be small and the classical MC simulation methods used here are valid. The equilibrium lattice constants are plotted in Fig. 1. The QH results are in excellent agreement with the MC values. The LH values are somewhat larger than the MC values, but the agreement is still good considering the simplicity of the calculations. In the Appendix, a method based on a model density of states is discussed. The lattice constants predicted by this method are essentially the same as those

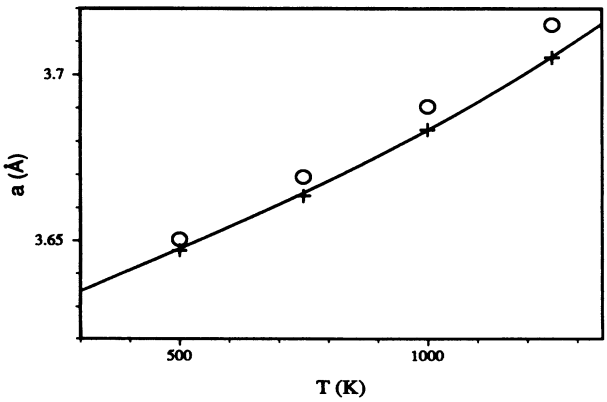

FIG. 1. The equilibrium lattice constants computed for the EAM model of Cu computed by MC (solid line), QH (pluses), and LH (circles) methods. The solid line is a fit through the MC data and the other data are representative points.

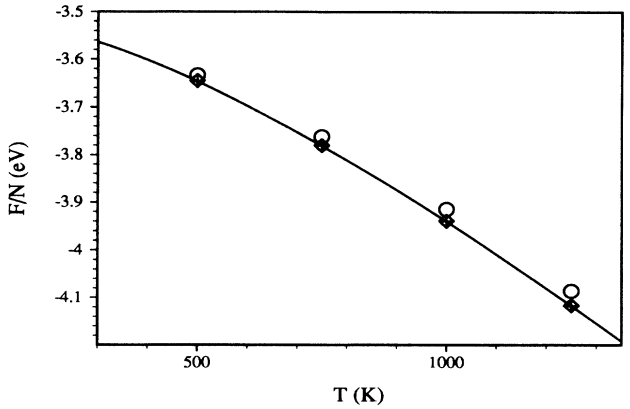

FIG. 2. The free energy of bulk fcc Cu as calculated by MC (solid line), LH approximation (circles), QH approximation (pluses), and the model density of states discussed in the Appendix (diamonds). Note that the solid line is a fit through the MC data, the other data are at representative points and the circles and diamonds are superimposed.

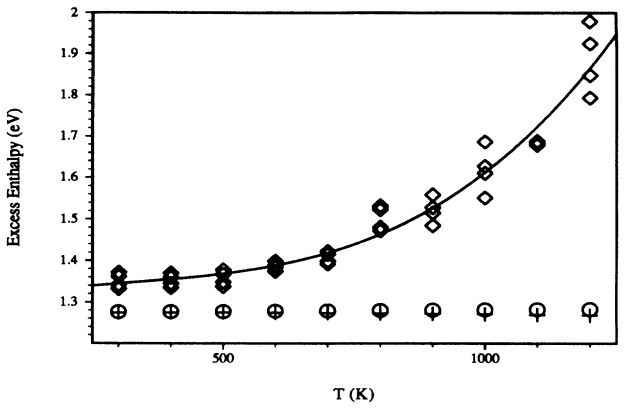

FIG. 3. The excess enthalpy of a monovacancy in Cu. The diamonds are the raw MC results obtained as the difference between two simulations with and without a vacancy at each temperature. The solid line is a fit to the MC data by a cubic polynomial. The pluses are the QH method results and the circles are the LH method results.

predicted by the LH method.

The free energies are plotted in Fig. 2. Again note that the QH results are in excellent agreement with the MC values. This is consistent with the earlier results of Foiles and Adams.[9] In this plot, both the values from the LH method and model density of states discussed in the Appendix are presented since the differences between the two approaches do not cancel out in the computation of the total free energy. Note that the LH model consistently overestimates the free energy while the model density of states produces results that are essentially the same as those obtained with QH calculations.

These bulk results indicate that QH calculations provide an excellent description of the thermodynamics of the ideal bulk solid and the model density of states leads to excellent predictions of the bulk thermodynamic properties. The LH model is somewhat less accurate, but still provides reasonable results and a faithful description of the trends. It should be noted that for the calculation of free energies, the model density of states does not require more computational effort than the LH method since both use the eigenvalues of the 3×3 matrices as inputs.

B. Vacancy

The first defect case is the monovacancy in Cu. The MC results were obtained as follows. First, the FL method was used to determine the free energy at 500 K. At higher temperature, it was found that the integration over λ in Eq. (2) was problematic because the integrand diverged at $\lambda=1$ due to the onset of diffusion during the course of the simulation. The excess enthalpy was then computed as a function of temperature using standard MC techniques. The results are shown in Fig. 3. Note that there is substantial scatter in the values. This is due to the fact that the vacancy formation energy is less than the variation of the total energy of the system in the simulations at higher temperatures. The general behavior of the excess enthalpy from the simulations is clear, though. The solid line is a fit to the data by a cubic polynomial. The excess free energy of the vacancy is computed by thermodynamic integration, Eq. (1), using the fit polynomial. The resulting free energy is plotted in Fig. 4.

The QH and LH values of the excess enthalpy are also plotted in Fig. 3. Note that both of these methods yield excess enthalpies which are almost independent of temperature, while the MC values increase with temperature especially for temperatures above around 600 K. The excess free energies are plotted in Fig. 4. Note that both of these methods predict a smaller temperature variation than found in the MC results. This is consistent with the smaller excess enthalpies. Also, note that the LH method predicts a smaller temperature variation than is predicted by the full QH calculation. The origin of the disagreement between the harmonic methods and the MC results

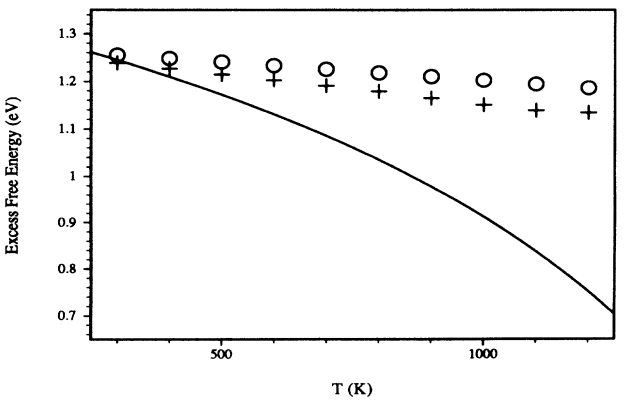

FIG. 4. The excess free energy of a monovacancy as computed by MC simulations (solid line), QH method (pluses), and LH method (circles).

is not completely clear. The loss of local inversion symmetry at the defect means that anharmonic corrections should be much larger than in the bulk as discussed earlier. In addition, at the highest temperatures, the vacancy is seen to diffuse during the course of the simulation, so the onset of diffusion behavior contributes at least near the melting point.

C. Surfaces

The surface excess enthalpy and surface free energy of Cu(100) have been computed. (In defining the surface excess enthalpy, the excess number of the surface is chosen to be zero.) The results for the excess enthalpy are shown in Fig. 5. The solid line represents a fit of a cubic polynomial to the MC data. Note that there is substantially less scatter in the raw MC data than in the case of the monovacancy. Like the monovacancy case, the MC values of the excess enthalpy deviates above the approximate treatments for high temperatures. Figure 6 plots the surface free energy as a function of temperature for the three methods. The free energy from the MC calculations is lower at high temperatures than from either the QH or LH methods. In particular, note that the LH and QH methods underestimate the temperature variation by a factor of about 3 or 2, respectively.

There is an unexpected aspect of the QH and LH results, though. While the QH method is in better agreement with the MC results for the free energy, it is in poorer agreement for the excess enthalpy. The poorer results of the QH method for the enthalpy compared to the LH method are due to the different treatments of the structure in the LH and QH methods. In the QH calculations presented here, the positions are the relaxed zero-temperature positions scaled by the bulk thermal expansion. The LH method minimizes the free energy with respect to the atomic positions. To see the effect of this difference, the interlayer spacings for the QH calculations

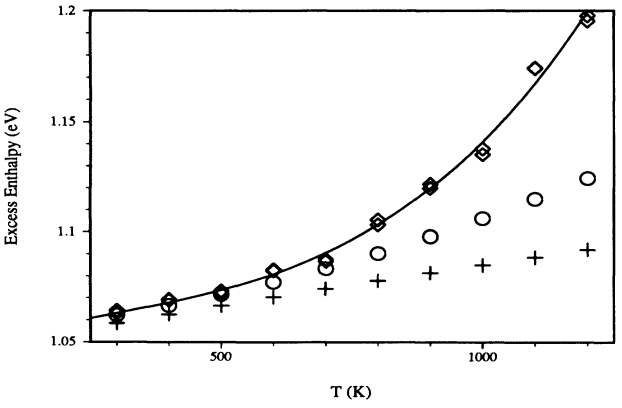

FIG. 5. The excess enthalpy of a Cu(100) surface in eV per cubic unit cell. The diamonds are the raw MC results and the solid line is a fit to the data by a cubic polynomial. The pluses are the QH method results and the circles are the LH method results.

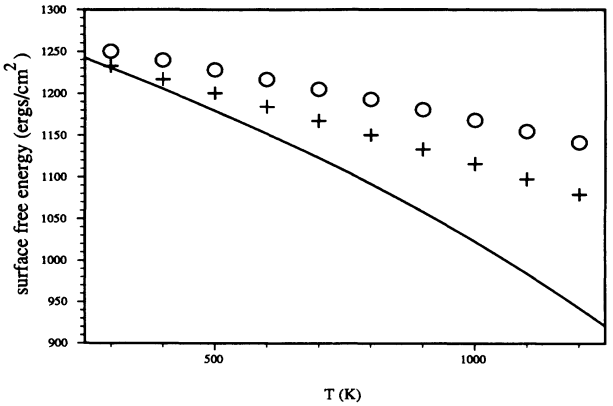

FIG. 6. The surface free energy of a Cu(100) surface as computed from the MC simulations (solid line), QH method (pluses), and LH method (circles).

were adjusted manually to find a free-energy minimum at 1000 K. (Only the first two interlayer spacings were adjusted.) The free-energy minimum was found for an increase in z_{12} of 0.013 Å and a decrease of z_{23} of 0.002 Å relative to the spacings obtained by expanding the zero-temperature result. This relaxation decreased the free energy of the surface by 0.0005 eV per cubic unit cell. This corresponds to a change in the surface free energy of about 0.5 ergs/cm^2. Thus, ignoring the relaxation is a good approximation for the free energy. In contrast, the enthalpy change associated with this relaxation is an increase of 0.010 eV per cubic unit cell. The enthalpy is more severely affected than the free energy since it is the free energy that is a minimum at the correct atomic positions. Thus, approximations to the positions yield errors in the free energy that are second order in the displacements. However, the enthalpy is not a minimum, so errors in the displacements lead to first-order errors in the enthalpy. Thus, the treatment of the displacements in the QH calculations used here is adequate for the determination of the free energy, but is less satisfactory for the other thermodynamic functions such as the enthalpy or energy.

It is also interesting to compare the various predictions for the change in interlayer spacings. The values of Δz_{12}, the difference in the first interlayer spacing at 1000 K relative to the bulk interlayer spacing at that temperature, are -0.008 Å for the LH method, -0.013 Å for the QH method, and -0.008 ± 0.002 Å for the MC simulations. (For comparison, Δz_{12} is -0.026 Å at zero temperature.[20]) The good agreement between the LH and MC results is fortuitous. The QH method gives the best answer within the harmonic approximation. Thus, the larger interlayer spacing found in the MC simulations compared to the QH results is a reflection of anharmonicity. The larger interlayer spacing of the LH method relative to the QH method reflects errors in the LH treatment of the harmonic approximation and is the origin of the larger excess enthalpy computed by the LH method. It should be noted, though, that all of the approaches

give similar answers, namely, that the first interlayer spacing is increasing with temperature more rapidly than the bulk.

It is interesting to note that the onset of anharmonicity at around half of the melting point has been observed previously in both experimental[25] and theoretical[26,27] investigations of surface vibrations. The low-energy electron diffraction (LEED) studies by Cao and Conrad[25] show an increase in the thermal expansion of the Ni(100) and (110) surfaces. They also show an decrease in the diffraction intensity with increasing temperature that is much stronger than is predicted based on a harmonic model. This indicates that the surface is behaving anharmonically. These observations have been confirmed by molecular-dynamics simulations.[26,27]

D. Grain boundary

As a test of an internal interface, the free energy of a symmetric tilt boundary was determined. The boundary considered is a $\Sigma 5(310)/[001]$ symmetric tilt boundary. This boundary is obtained by rotating the two crystals around [001] directions such that {310} planes are parallel to the boundary in both crystals. (Each crystal is rotated by $\frac{1}{2}$ of 36.87°.) The calculated zero-temperature structure of this boundary is shown in Fig. 7. The calculations were performed in a slab geometry with periodic boundary conditions in the plane of the boundary and free surfaces normal to the boundary. In order to subtract out the bulk and surface quantities, corresponding calculations were also performed for slabs of the same dimensions and number of atoms but not containing a grain boundary. Since the surfaces of the two slabs are the same, subtracting the slab results from the grain boundary results yields the excess associated with the boundary.

The excess enthalpy of the grain boundary as a function of temperature is plotted in Fig. 8. The results are qualitatively similar to those obtained for the Cu(100) surface discussed above. The two harmonic approaches, LH and QH, show substantially less temperature variation than is found in the MC results. Also, the LH results again show a larger temperature variation than the QH data reflecting the fact that the QH calculations do not incorporate temperature variations of the structure.

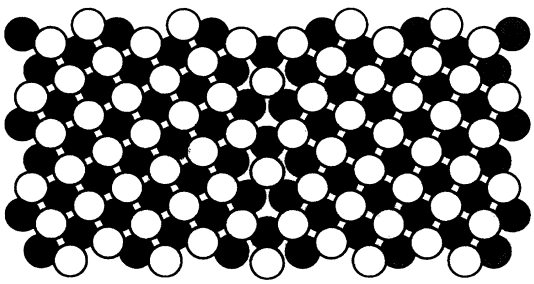

FIG. 7. Zero-temperature structure of the $\Sigma 5$ (310)/[001] symmetric tilt boundary. The shading of the atoms differentiates the position of the atom normal to the figure.

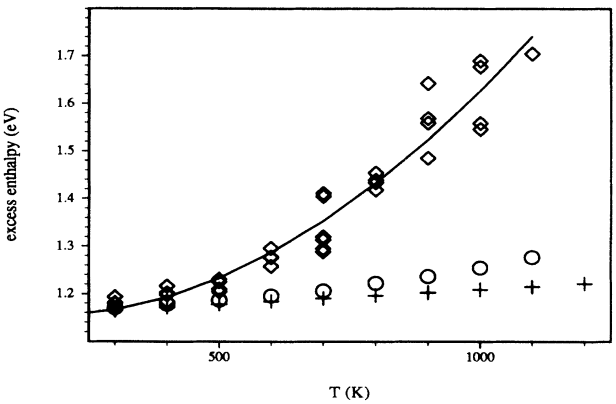

FIG. 8. The excess enthalpy of a Cu $\Sigma 5$ (310)/[001] symmetric tilt boundary in eV per unit cell of the boundary. The diamonds are the raw MC results and the solid line is a fit to the data by a cubic polynomial. The pluses are the QH method results and the circles are the LH method results.

The main difference between these grain boundary results and the surface results is that the magnitude of the deviation of the MC results from the harmonic methods is larger. This suggests that the potential seen by the atoms is more anharmonic at the grain boundary than at the surface. It also reflects the observation that there is substantial motion of the atoms at the grain boundary during the simulations. This suggests the onset of diffusive contributions to the energetics.

The interfacial free energy of the grain boundary is plotted in Fig. 9. Again, the results are qualitatively similar to those found for the (100) surface with the deviations being of a larger magnitude. Note that near the melting point, the MC results for the interfacial free energy differ from the harmonic results by about a factor of 2. This casts serious doubt on the ability of harmonic-based methods to accurately predict the high-temperature thermodynamics of internal interfaces.

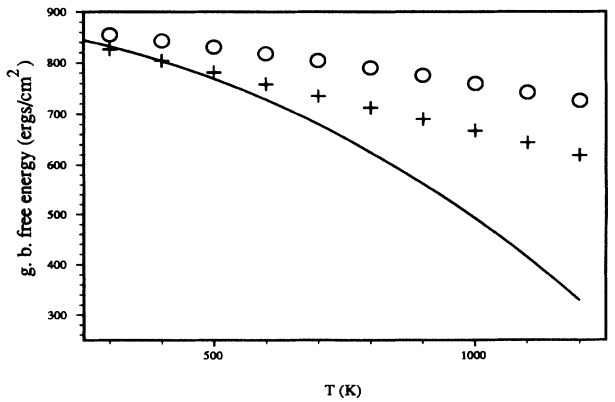

FIG. 9. The interfacial free energy of a Cu $\Sigma 5$ (310)/[001] symmetric tilt boundary as computed from the MC simulations (solid line), QH method (pluses), and LH method (circles).

IV. DISCUSSION

The LH and QH methods both give a good description of the thermodynamic properties of the bulk fcc crystal with EAM potentials for Cu. This is consistent with previous observations. However, for the potential studied here, both of these methods based on the harmonic approximation deviate significantly from the MC results for defects at temperatures above roughly half of the melting point. This deviation is most apparent in the excess enthalpy where the MC results show a substantial increase above this point while the harmonic-based methods show smaller temperature variations which are roughly linear. The fact that this general behavior was observed in all cases studied here suggests that it is not restricted to a specific type of defect. This increase in the excess enthalpy may result either from the onset of anharmonic effects and/or from the onset of diffusive processes. The presence of the latter can be deduced from the direct observation of diffusion in the simulations at high temperatures. In particular, some of the atoms in the vicinity of the defect exchange lattice sites during the course of the simulations at high temperature and these exchanges are found to occur for approximately the same range of temperatures as the above deviations from harmonic behavior.

The increase in the excess enthalpy at high temperatures in the MC results leads to a decrease in the free energies associated with these defects. As a result, both of the harmonic methods lead to a substantial underestimation of the temperature variation of the defect-free energies relative to the full MC results. In addition, it should be noted that the LH approximation also consistently underestimates the temperature variation of the defect-free energy relative to the QH method.

The results obtained here are at variance with the earlier results for the free energy of a monovacancy described by a Morse potential.[10] In that study, the free energy obtained from the LH method agreed with the MC results to within ~ 0.04 eV up to 75% of the melting point. The reason for the different levels of agreement in the two cases will be the subject of future investigations. The present results do indicate that the use of the QH method or methods derived from them such as the LH method for the calculation of defect thermodynamics may result in significant quantitative errors at high temperatures in some cases. For the potential studied here, namely, Cu modeled by EAM potentials, these methods begin to break down at roughly half of the melting point. Therefore, care must be taken to assure the applicability of harmonic methods for the case of interest.

ACKNOWLEDGMENTS

The code used for the LH calculations was developed by J. D. Rittner, Northwestern University. This work was supported by the U.S. Department of Energy, Office of Basic Energy Sciences, Division of Materials Science.

APPENDIX

The LH approximation models the density of states as a δ function. This leads to the expression for the free energy given in Eq. (7). The actual density of states of a metal has significant width and one might expect to obtain a better description of the free energy with a more physical model of the density of states. The density of states can be treated as having the following model form:

$$n_{i\alpha}(\omega)=\frac{4\omega^2}{\pi(\mu_{i\alpha}^{(2)})^2}(2\mu_{i\alpha}^{(2)}-\omega^2)^{1/2} . \tag{A1}$$

This expression has the correct behavior at the band edges and provides a reasonable approximation to the full density of states of a crystal. In the classical limit, the value of F/k_BT predicted by this model density of states differs from the LH result by a constant,

$$\frac{F_{\text{model}}}{k_BT}-\frac{F_{\text{LH}}}{k_BT}=(\tfrac{1}{4}-\tfrac{1}{2}\ln 2)\approx -0.0966 . \tag{A2}$$

The bulk free energies predicted by this model are also presented in Fig. 2. The results are in much better agreement with the QH and MC values then is the LH model.

Sutton[15] proposed a very similar model of the density of states earlier. There are two differences. First, the local density of states is treated on a per atom rather than per mode basis. The second, and more important, difference concerns the normalization of the second moment and of the density of states. The second moment values differ by a factor of 3 for a perfect crystal. The current model has the advantage that the second moment corresponds to the width of the density of states. Also, as was observed by Rickman and Srolovitz,[17] the model proposed by Sutton yields free energies in poorer agreement with QH results than the LH model while the model proposed here predicts better agreement with the QH results than the LH model.

Finally, one could also model the density of states by a Debye[28] form with the prefactor and Debye frequency chosen to yield the correct normalization and second moment. This leads to results very similar to those found for the model density of states discussed above. In that case in the classical limit, the constant corresponding to Eq. (A2) is $[\frac{1}{2}\ln(\frac{5}{3})-\frac{1}{3}]\approx -0.0779$. This leads to slightly poorer agreement with the QH and MC results than does the above model but still yields better agreement than the LH model.

[1]B. Widom, J. Chem. Phys. **39**, 2808 (1963).
[2]I. R. McDonald and K. Singer, Discuss. Faraday Soc. **43**, 40 (1967); I. R. McDonald and K. Singer, J. Chem. Phys. **47**, 4766 (1967); **50**, 2308 (1969).
[3]J. P. Valleau and G. M. Torrie, in *Modern Theoretical Chemistry*, edited by B. J. Berne (Plenum, New York, 1976), Vol. 5.
[4]D. Frenkel and A. J. C. Ladd, J. Chem. Phys. **81**, 3188 (1984).
[5]J. Q. Broughton and X. P. Li, Phys. Rev. B **35**, 9120 (1987).
[6]J. M. Rickman and S. R. Philpot, J. Chem. Phys. **95**, 7562 (1991).
[7]J. M. Rickman, R. Najafabadi, L. Zhao, and D. J. Srolovitz, J. Phys. Condens. Matter **4**, 4923 (1992).
[8]A. A. Maradudin, E. W. Montroll, G. H. Weiss, and I. P. Ipatova, *Theory of Lattice Dynamics in the Harmonic Approximation*, 2nd ed. (Academic, New York, 1971).
[9]S. M. Foiles and J. B. Adams, Phys. Rev. B **40**, 5909 (1989).
[10]R. LeSar, R. Najafabadi, and D. J. Srolovitz, Phys. Rev. Lett. **63**, 624 (1989).
[11]A. P. Sutton, Philos. Mag. A **60**, 147 (1989).
[12]R. Najafabadi, D. J. Srolovitz, and R. LeSar, J. Mater. Res. **5**, 2663 (1990); **6**, 999 (1991).
[13]R. Najafabadi, H. Y. Wang, D. J. Srolovitz, and R. LeSar, Acta Metall. Mater. **39**, 3071 (1991).
[14]H. Y. Wang, R. Najafabadi, D. J. Srolovitz, and R. LeSar, Phys. Rev. B **45**, 12 128 (1992).
[15]A. P. Sutton, Philos. Trans. R. Soc. London Ser. A **341**, 233 (1992).
[16]J. D. Rittner, S. M. Foiles, and D. N. Seidman (unpublished).
[17]J. M. Rickman and D. J. Srolovitz, Philos. Mag. A **67**, 1081 (1993).
[18]L. Zhao, R. Najafabadi, and D. J. Srolovitz, Model. Simul. Mater. Sci. Eng. **1**, 539 (1993).
[19]M. S. Daw and M. I. Baskes, Phys. Rev. B **29**, 6443 (1984).
[20]S. M. Foiles, M. I. Baskes, and M. S. Daw, Phys. Rev. B **33**, 7983 (1986); **37**, 10 387 (1988).
[21]M. S. Daw, S. M. Foiles, and M. I. Baskes, Mater. Sci. Rep. **9**, 251 (1993); S. M. Foiles, in *Equilibrium Structure and Properties of Surfaces and Interfaces*, edited by A. Gonis and G. M. Stocks (Plenum, New York, 1992).
[22]W. C. Swope and H. C. Anderson, Phys. Rev. A **46**, 4539 (1992).
[23]For example, N. W. Ashcroft and N. D. Mermin, *Solid State Physics* (Holt, Rinehart, and Winston, New York, 1976).
[24]F. Cryot-Lackmann, J. Phys. Chem. Solids **29**, 1235 (1968).
[25]Yijian Cao and E. Conrad, Phys. Rev. Lett. **65**, 2808 (1990); **64**, 447 (1990).
[26]L. Yang, T. S. Rahman, and M. S. Daw, Phys. Rev. B **44**, 13 725 (1991); L. Yang and T. S. Rahman, Phys. Rev. Lett. **67**, 2327 (1991).
[27]Y. Beaudet, L. J. Lewis, and M. Persson, Phys. Rev. B **47**, 4127 (1993); in *Materials Theory and Modelling*, edited by J. Broughton, P. Bristowe, and J. Newsman, MRS Symposia Proceedings No. 291 (Materials Research Society, Pittsburgh, 1993).
[28]S. M. Foiles and M. S. Daw, Phys. Rev. B **38**, 12 643 (1988).

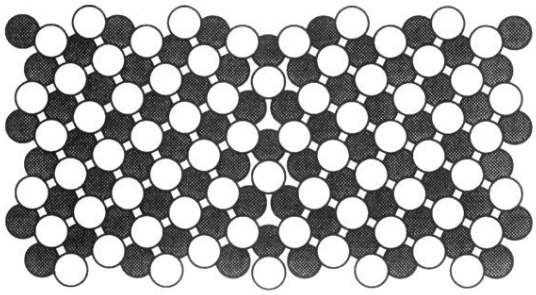

FIG. 7. Zero-temperature structure of the $\Sigma 5$ (310)/[001] symmetric tilt boundary. The shading of the atoms differentiates the position of the atom normal to the figure.